Earth Surface Processes and Landforms
Earth Surf. Process. Landforms (in press)
Published online in Wiley InterScience
(www.interscience.wiley.com) **DOI:** 10.1002/esp.1489

Fluvial thermal erosion: heat balance integral method

R. Randriamazaoro, L. Dupeyrat,* F. Costard and E. Carey Gailhardis
UMR8148-IDES, CNRS-UPS, Université Paris-Sud, Orsay, France

**Correspondence to: L. Dupeyrat, UMR8148-IDES, CNRS-UPS, bâtiment 509, Université Paris-Sud, 91405 Orsay, France. E-mail: dupeyrat@geol.u-psud.fr*

Received 20 July 2005;
Revised 21 September 2006;
Accepted 20 November 2006

Abstract

In periglacial regions, frozen river banks are affected by thermal and mechanical erosion. In Siberia, bank retreats of up to 40 m per year are observed. This thermal erosion occurs during a few weeks, at springtime, for high enough water temperatures and river discharges. Until now, models of thermal erosion have been based on the assumption of a constant thermal erosion rate. We have developed a more general model at variable rate, whose solution is calculated using the integral method. Results of this model are compared with experiments, carried out in a cold room. A hydraulic channel allows measurements of the thermal erosion rate of a ground ice sample subjected to a turbulent water flow. Once validated, the model is applied to the periglacial river study case. The model has contributed to better understanding of the roles of each parameter during the thermal erosion process. High water temperature, discharge and ice temperature produce major thermal erosion, whereas the ice content in the soil tends to slow down the thermal erosion process. The effects of water temperature are predominant. An acceleration phase characterized by an increase of the thermal erosion rate occurs at the beginning of the thermal erosion process. The duration of such an acceleration phase is systematically studied. A relatively long acceleration phase is related to a low ablation rate. During the flood season, when the water temperature is increased to 18 °C, this acceleration phase lasts only a few minutes. However, for data typical of periglacial rivers, when the water temperature is close to the melting point, the acceleration phase can last a few days.

Keywords: thermal erosion; permafrost; periglacial river; phase change

Introduction

Permafrost and ice underlie about 25 and 10%, respectively, of the earth's land surface. In periglacial environments, the term permafrost describes the condition of earth materials that remain below 0 °C continuously for at least two years. Its persistence or disappearance is highly dependent on climate change, environment processes and human activities. The Yakutia region (Central Siberia) is a particularly interesting area for the breakup of rivers and for its lowest temperature records as well as for its maximum thickness of permafrost. The average thickness of the Siberian permafrost is about 350 m (Anisimova *et al*., 1973) but the maximum thickness of permafrost is 1450 m. The temperature of continuous permafrost at the depth of minimum annual seasonal change varies from −5 to −13 °C (Péwé, 1991).

The Lena river is the largest scale fluvial system of Siberia (Yang *et al*., 2002). The total length of the Lena river exceeds 4000 km and the width of the floodplain can reach 25 km downstream of Yakutsk (62° N, 130° E; Shiklomanov *et al*., 2000). The width of the channels varies between several hundred metres and three kilometres. These multiple channels enclose large forested islands from 1 to 5 km long and large sandy bars (Anisimova *et al*., 1973; Gautier and Costard, 2000).

During springtime, most periglacial rivers, including the Lena river in Siberia, exhibit high discharge rates and high temperatures (Antonov, 1960; Gordeev and Sidorov, 1993; Yamskikh *et al*., 1999). The Lena River and its tributaries can be divided into two classes, (1) the Lena basin outlet and (2) the southern sub-basins (Aldan, Upper Lena, Vilui

valley). In the first case, a relatively low temperature variation and a high discharge variation characterize the Lena basin outlet. The stream temperature varies from 0 °C to 14 °C and the discharges can reach 100 000 $m^3 s^{-1}$ in early June (Gautier *et al*., 2003; Liu *et al*., 2005; Yang *et al*., 2005). In the second case, the southern sub-basins are characterized by relatively high temperature and low discharge. For these rivers, water temperatures are up to 4 °C higher than those over the Lena outlet (Liu *et al*., 2005) and can reach 18 °C. The discharges are about ten times smaller than in the Lena basin outlet (Liu *et al*., 2005; Yang *et al*., 2005).

During the break-up and flood seasons, the river water induces the propagation of a thawing line within the frozen riverbank. At the latitude of Yakutsk, most river banks are made of non-cohesive materials (sand and silt materials) with different ice contents (Anisimova *et al*., 1973). Thawing of the ice (for any ice content) within a porous medium reduces the strength of the thawed sediments and produces easily removable uncemented ground (Jahn, 1975). During the thawing period, with a relatively high discharge, the thawed sediments are swept away (Gautier and Costard, 2000). In this typical situation, the water flow in permanent contact with frozen river banks induces a combination of thermal and mechanical erosion. The erosion of riverbanks can be as high as 40 m/year (Are *et al*., 1983; Gautier *et al*., 2003). In contact with water, they are warmed and lose their strength progressively due to the melt of ice. These processes can intensify mechanical erosion such as collapse or removal of sediments. The major factors controlling this process are the water temperature, the flow discharge, the ice temperature and the level of massic ice content (Costard *et al*., 2003).

The thermal erosion process falls into the category of a heat-conduction problem involving a phase change. This problem is non-linear because it involves a moving boundary (interface between solid and liquid) whose location is unknown at first sight. Until now, models of thermal erosion based on the assumption of a constant melting rate for a constant convective flux at the interface have been used to study thermal erosion of ice and permafrost (Costard and Aguirre-Puente *et al*., 1994). In this case, an analytical solution of both the conductive heat equation in permafrost and heat flux balance at the permafrost/water flow interface can be formulated (Soodak, 1943; Landau, 1950; Carslaw and Jaeger, 1959). Such a model at a constant rate of melting has been validated by numerous laboratory experiments. Nevertheless, for particular values of water temperature, water discharge and ice temperature, some slight variations have been observed in measurements at the beginning of the process.

The first impetus of this paper is to develop a model of thermal erosion of permafrost without the simplified assumption of a constant melt rate. Results of this model will be compared with experimental data (following section). Once validated, the model will be applied to the Siberian river case. The second aim of this study is to determine the benefit of a model with variable melt rate compared with the simplified model with constant melt rate, according to the temperatures, the discharges and the massic ice content.

The Ablation Model

In contact with a turbulent water flow, the ice or the permafrost warms and melts since its temperature has reached melting point (T_m = 0 °C). One of the main characteristics of phase change problems is the existence of a moving interface between the solid and the fluid phase. Such a process can be characterized by the variation of the interface with time, and eventually the temperature distribution in the solid.

In order to study the thermal erosion process, a semi-infinite ice or permafrost sample in contact with a turbulent water flow (Reynolds number Re > 2000) may be considered (Figure 1). The sample is initially ($t = t_0$) at a uniform temperature (T_∞). The water flow is maintained at a constant temperature (T_L) and at a constant degree of turbulence (Re). It is inferred that all the melt is immediately swept away by mechanical action. The instantaneous location of the moving interface and the thickness of the thermal boundary layer in the solid are represented by $s(t)$ and $\delta(t)$, respectively.

Mathematical model

During a very short transient phase, the solid/liquid interface is heated until it reaches the melting temperature ($t_0 < t < t_i$). Thermal erosion is active since the interface has reached the melting temperature ($t > t_i$). Inside the solid, the heat transfer occurs by conduction:

$$\frac{\partial T}{\partial t} = \alpha \frac{\partial}{\partial x}\left(\frac{\partial T}{\partial x}\right) \quad x \geq s(t) \quad \forall t \tag{1}$$

where α [m^2/s] is the thermal diffusivity in the solid.

DOI: 10.1002/esp

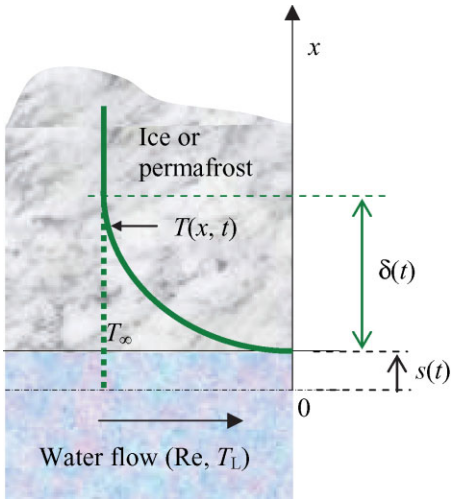

Figure 1. Semi-infinite sample of permafrost initially at a uniform temperature (T_∞) in contact with a turbulent water flow (Re > 2000, T_L). Location of the moving interface at $t = t_0$ (0) and $t > t_0$ ($s(t)$). Thickness of the thermal boundary layer in the permafrost ($\delta(t)$). This figure is available in colour online at www.interscience.wiley.com/journal/espl

At the solid–liquid interface, the heat flux provided by the water flow must equal the conductive heat flux in the solid added to the latent heat absorbed by melting.

$$h(T_L - T_f) = \rho L \frac{\partial s}{\partial t} - k\left(\frac{\partial T}{\partial x}\right)_{x=s} \qquad x = s(t) \quad t > 0 \tag{2}$$

where L [J kg^{-1}] is the latent heat of melting and h [W m^{-2} s^{-1}] is the heat transfer coefficient.

The sample is initially ($t = t_0$) at a uniform temperature (T_∞). After the transient phase ($t > t_i$), the moving interface ($x = s(t)$) is at the melting temperature (0 °C), whereas far from it the sample remains at its initial temperature (T_∞):

$$\begin{aligned} &T(x, t_0) = T_\infty \qquad \forall x \\ &T(x, t) = 0\ ^\circ\mathrm{C} \quad x = s(t) \quad t > t_i \\ &T(x, t) = T_\infty \qquad x \to \infty \quad \forall t > 0 \end{aligned} \tag{3}$$

Resolution by the heat balance integral method

Goodman's solutions. The 'heat-balance integral method' consists of integrating the heat conduction equation over the thermal layer $\delta(t)$ (Equation (4) below). It is based on the assumption that a quadratic law, fulfilling the boundary conditions, represents the temperature distribution in the solid (Equation (5) below). The parabolic shape of the temperature profile is justified by the review of exact solutions that have been developed for related problems. For example, the steady internal heating problem for a conducting material in contact with a uniform fluid flow is solved analytically and results in a parabolic temperature distribution (Bejan, 1993). The assumption of a quadratic boundary layer temperature is also commonly used for unidirectional conductive internal heating problems with temperature dependent heating or for two-dimensional conductive internal heating (Bejan, 1993).

$$\frac{\partial}{\partial t}\int_s^\delta T dx = \alpha\left[\left.\frac{\partial T(x, t)}{\partial x}\right|_{x=\delta} - \left.\frac{\partial T(x, t)}{\partial x}\right|_{x=s}\right] \tag{4}$$

Applying the boundary conditions (3), we obtained

DOI: 10.1002/esp

$$T(x,t) = T_\infty\left[-2\left(\frac{x-s}{\delta-s}\right)+\left(\frac{x-s}{\delta-s}\right)^2\right] \quad s(t) < x < \delta(t) \quad t > 0 \tag{5}$$

$$\frac{\partial T}{\partial x} = 0 \qquad x \geq \delta(t)$$

After substituting the temperature distribution in Equation (2), integrating Equation (4) and applying boundary and initial conditions (3), solutions in adimensional form are obtained (Goodman, 1958):

$$(\Sigma) = \begin{cases} \Omega = -\frac{1}{3}\left[\xi - 2 + 2\left(1+\frac{1}{St}\right)\mathrm{Log}\frac{St}{2}\left(2\left(1+\frac{1}{St}\right)-\xi\right)\right] \\ S = -\frac{1}{3}\left[\xi - 2 + \frac{2}{St}\mathrm{Log}\frac{St}{2}\left(2\left(1+\frac{1}{St}\right)-\xi\right)\right] \end{cases} \tag{6}$$

with

$$St = \frac{Cp(T_\infty - T_f)}{L} \tag{7}$$

where ξ and S are unknowns for a given Ω and St is the Stefan number. Cp [J.kg−1.°C−1] is the specific heat.

The adimensional parameters involved in the equation system are the time Ω (8), the location of the interface S (9) and the thermal boundary thickness ξ (10).

$$\Omega = \frac{h^2(T_L - T_f)^2}{\rho k L T_\infty}t \tag{8}$$

$$S = \frac{h(T_L - T_f)}{kT_\infty}s \tag{9}$$

$$\xi = \frac{h(T_L - T_f)(\delta - s)}{kT_\infty} \tag{10}$$

Analysis and resolution of Goodman's solutions

The equation system (Σ) is only valid where $\xi(t)$ belongs to the interval $E = [2;2(1 + 1/St)]$. The function $\xi(t)$ is monotonic and strictly increasing in this interval. A steady-state solution for $t \to \infty$ can be found easily because $\xi(t)$ tends towards a constant value $\xi_{lim} = 2(1 + 1/St)$ when t tends towards infinity (Equation (6)).

There are two ways to solve the equation system (Σ). The first way consists of calculating $\xi(t)$ at any time t. Afterwards, $\xi(\Omega)$ values will be substituted in the second equation of (Σ) to find $S(\Omega)$ by an approximate method. The second method consists of calculating t and s for any ξ belonging to the interval E by an exact resolution.

Our adimensional solutions $S(\Omega)$ of the equation system (Σ) are plotted (Figure 2), for specific values of Stefan numbers, in order to compare our results with those of Goodman (1958). Solutions for the constant-rate melting model (Aguirre *et al*., 1994; Costard *et al*., 2003) are also represented. Our results, those of Goodman (1958) and those obtained numerically by Landau (1950) are indistinguishable (Figure 2). Moreover, our solutions obtained with the integral method tend asymptotically towards the solutions of the constant-rate melting model.

Calculation of the location of the interface ($s(t)$) and the ablation rate (ds/dt)

The instantaneous melting rate is calculated from the adimensional thermal boundary thickness ξ solved from the equation system (6).

$$\frac{ds(t)}{dt} = \frac{h(T_L - T_f)}{\rho L}\left(\frac{\xi - 2}{\xi}\right) \tag{11}$$

DOI: 10.1002/esp

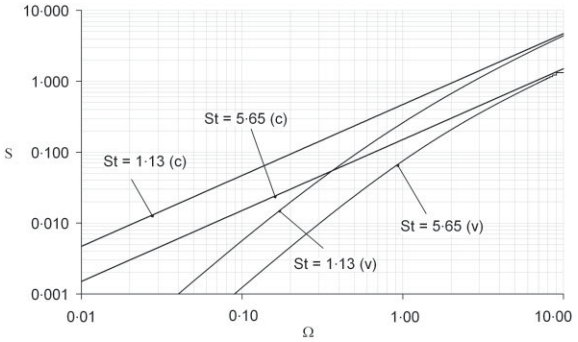

Figure 2. 'Adimensional' position of the interface versus 'adimensional' time, for different Stefan numbers. (c) constant-rate model; (v) variable-rate model.

By substituting ξ_{lim} in the melting rate Equation (11), the steady state melting rate is obtained:

$$\left(\frac{\mathrm{d}s}{\mathrm{d}t}\right)_{\text{lim}} = \frac{h(T_{\text{L}} - T_{\text{f}})}{\rho L}\left(\frac{1}{\text{St} + 1}\right) \tag{12}$$

The Goodman solutions S and ξ ((9) and (10)) allow determination of the location of the interface ($s(t)$) and the ablation rate ($\mathrm{d}s/\mathrm{d}t$).

The convective heat transfer coefficient h is linked to the water temperature and the level of turbulence water flow (Re). The convective heat transfer coefficient is calculated from the Nusselt number (13), which is determined from an empirical relation (14).

$$\text{Nu} = \frac{h.L}{k} \tag{13}$$

$$\text{Nu} = A\text{Pr}^{\alpha}\text{Re}^{\beta} \tag{14}$$

where Pr and Re are respectively the Prandtl and Reynolds numbers. A, α and β are empirical coefficients, which depend on the flow regime and geometry.

Results

Experimental set-up

In order to validate this mathematical approach, experiments have been carried out in a cold room. These experiments consist of measuring the erosion rate of ice samples (40 cm × 20 cm × 10 cm) by a turbulent water flow confined in a hydraulic channel. The hydraulic channel is a rectangular cross section tube 2·5 m long by 20 cm across and equipped with a pump for water recycling purposes. The sample is fixed on a vertical support and put in contact with the underneath turbulent water flow. The vertical support can slide downward along a linear steel track as fast as the erosion occurs, using a laser beam placed at the sample base. The laser apparatus is connected to a data acquisition system.

During these experiments, various water temperatures from 5 to 10 °C, ice temperatures from −7·5 to −10 °C and Reynolds numbers from 6300 to 15 900 are tested (Figure 3).

Figure 3 shows that the displacement of the interface is quasi-linear. It is very difficult to highlight the acceleration phase in the eroded thickness representation. The eroded thickness increases when the temperature of water, the Reynolds number and the temperature of the ice increase. The validation of the model is tested by the consistency between the experimental results and the theoretical predictions of the model (eroded thickness versus time of a permafrost sample subjected to a constant convective heat flux generated by a turbulent water flow).

DOI: 10.1002/esp

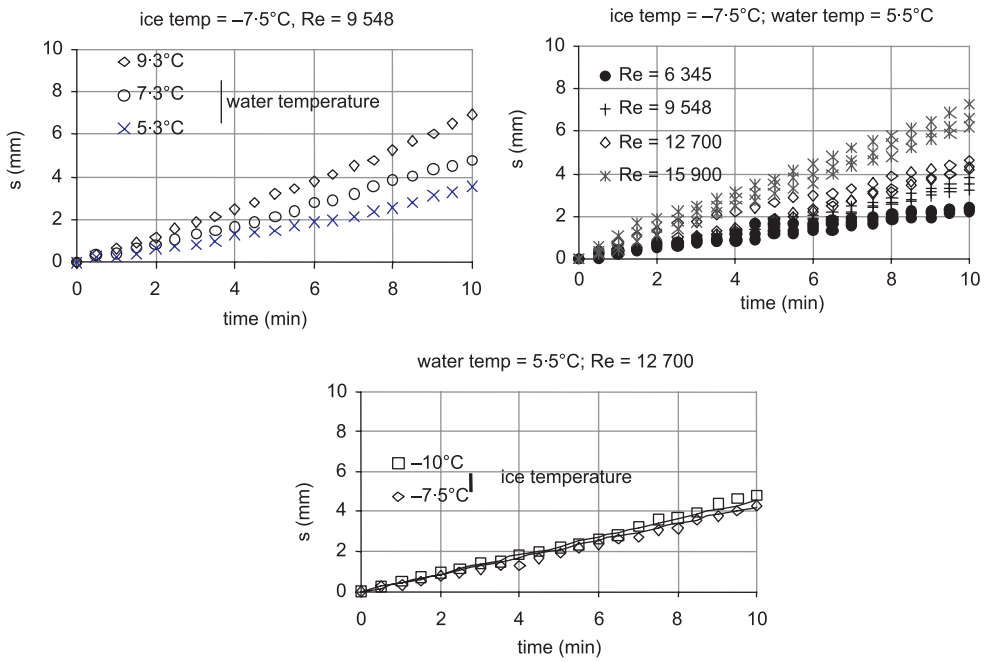

Figure 3. Experimental data. Effects of water temperature, discharge and ice temperature on the location of the moving surface $s(t)$. This figure is available in colour online at www.interscience.wiley.com/journal/espl

Duration of the acceleration phase

The ablation rate (ds/dt) (Figure 4) and the location of the moving interface ($s(t)$) (Figure 5) are calculated from the Goodman solutions.

Calculations are made for a reference case corresponding to ice initially at –7·5 °C, in contact with a water flow at 5·5 °C, with a Reynolds number equal to 15 900. Figure 4 shows that the ablation rate increases with time and progressively stabilizes. The limit corresponds to the ablation rate obtained by the constant-rate melting model. For example, it is equal to 0·7 mm min^{-1} for the reference case. The heat balance integral model shows that an acceleration phase of the thermal erosion rate exists at the beginning of the thermal erosion process. In our constant-heat-flux model, we consider that the convective heat flux at the water/permafrost interface is constant, as the water temperature and the flow discharge both remain constant during the whole process. Therefore, as the permafrost is progressively heated, the sensible heat must decrease. The heat flux balance (Equation (2)) implies that more energy is available for latent heat, providing an increase of the latent heat and therefore an acceleration of the melting rate. Quantifying this acceleration phase requires definition of the duration of the acceleration phase. A critical limit close to the asymptotic value must be chosen. Results are presented here for a critical value equal to 90% of the constant-rate melt model velocity. With this criterion, this acceleration phase lasts 6 min for the reference case.

Then, the effects of each parameter are studied separately for ice. The effects of the ice content are also studied by varying the ice content from 20% to infinity (ice) for a sandy permafrost (Figure 4). The increases of the ablation rate with the water temperature, ice temperature and Reynolds numbers (Figure 4) are in agreement with the experimental results (Figure 3).

When the Reynolds number increases, the ablation rate increases whereas the duration of the acceleration phase decreases. For example, for ice at –7·5 °C and water at 5·5 °C, if the Reynolds number is increased from 9500 to 19 000, the ablation rate is increased from 0·4 to 0·8 mm min^{-1} and the duration of the acceleration phase is decreased from 14 to 4 min. The ablation rate increases with the Reynolds number and the water temperature. Indeed, an increase of the thermal erosion rate of the permafrost is related to an increase of the convecting heat flux at its interface, which increases with the water temperature and the Reynolds number (Equations (2), (13) and (14)). This analysis also shows that the time to approach the asymptotic value reduces when the convecting heat flux increases. This means that the stabilization of the thermal profile in the half-infinite volume occurs faster. The ablation rate decreases when the ice content increases, as more latent energy is needed to melt the frozen ground.

DOI: 10.1002/esp

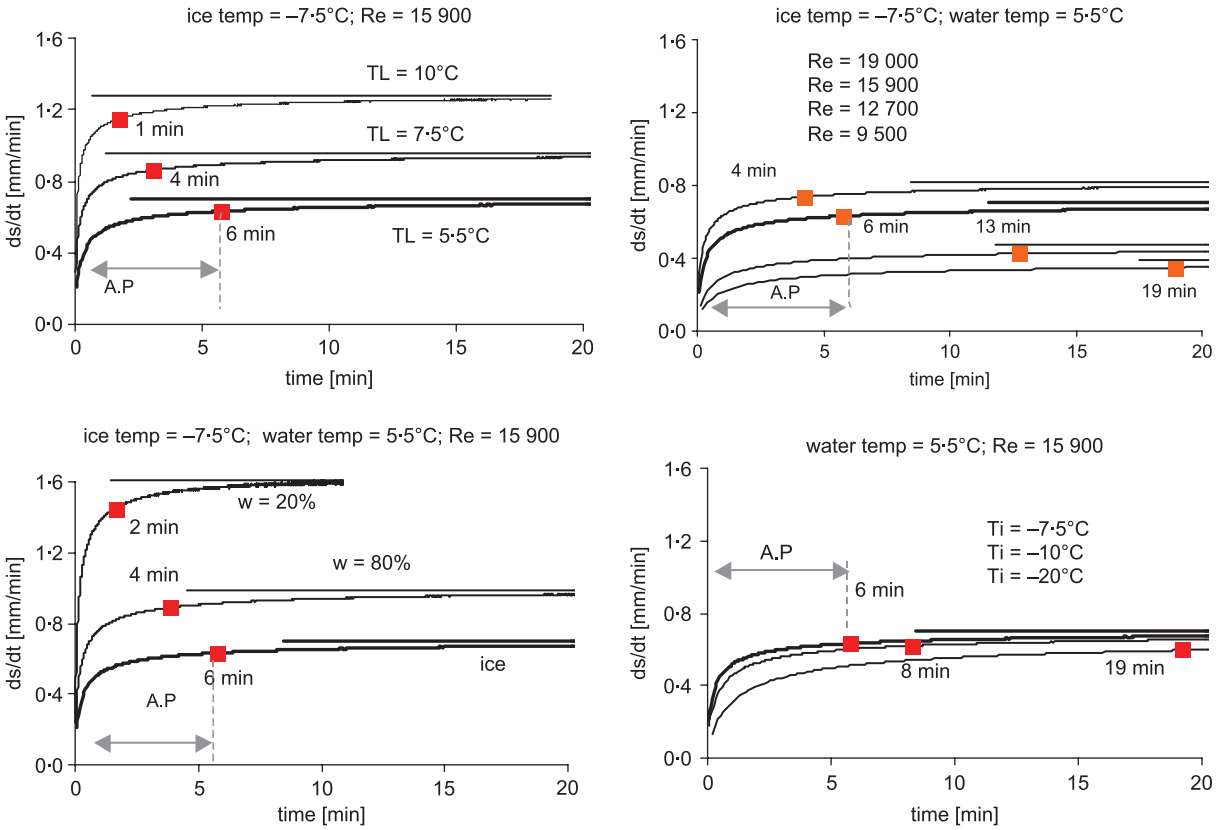

Figure 4. Evolution of the thermal erosion rate for different water temperatures, discharges, ice temperatures and ice contents. The reference case (bold line) corresponds to ice at –7·5 °C in contact with a water flow at 5·5 °C and a Reynolds number equal to 15 900. ■ corresponds to 90% of the final erosion rate and gives the duration of the acceleration phase (A.P.). This figure is available in colour online at www.interscience.wiley.com/journal/espl

In order to compare theoretical results with measurements, calculations of the location of the moving interface (Figure 5) are made for pure ice, a water temperature equal to 5 °C, an ice temperature equal to –7·5 °C and a Reynolds number ranging from 9500 to 19 000. Ho *et al.* (2000) have applied the integral method to solve the problem of cool thermal discharge from ice melting with removal of melt. Their calculated values of eroded thickness and our results are represented by curves with similar trends.

Thermal erosion: Application to a periglacial river bank

Our model of ablation at variable rate has been previously validated by experiments on ice samples and can be applied to permafrost, using appropriate properties of permafrost. For the calculation of the thermal erosion of a periglacial riverbank, the convective heat transfer coefficient may be estimated from the values of the river discharges, using the Manning equation (Equation (11)) (Costard *et al.*, 2003).

$$h = A\left[\left(\frac{\sqrt{s}}{n}\right)^{3/5} l^{3/5-\beta}\right]\left[\mathrm{Pr}^{\alpha}\frac{k_w}{\upsilon w^{\beta}}\right]Q^{\beta-3/5} \tag{20}$$

where n, S, l and k_w represent respectively the Manning roughness coefficient, the longitudinal slope, the width of the river and the thermal conductivity of the water. A typical river 10 km wide, with a longitudinal slope S equal to 0·0001 and a Manning coefficient equal to 0·1, is considered. In this application, we use the empirical coefficients experimentally determined by Lunardini *et al.* (1986) from water flowing over a horizontal ice sheet (A, α and β equal respectively to 0·0078, 0·3333 and 0·9270).

DOI: 10.1002/esp

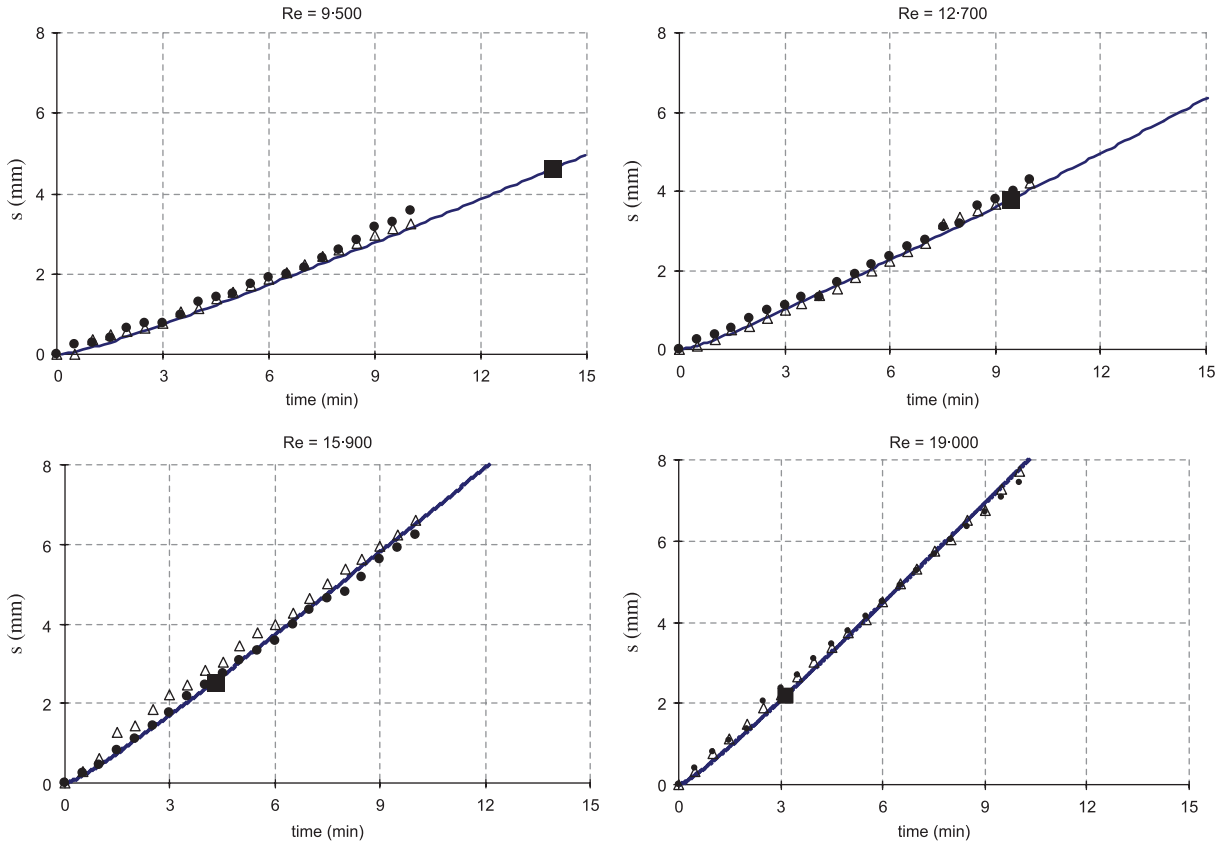

Figure 5. Eroded thickness versus time for pure ice. Comparison between the theoretical model (line) and the laboratory measurements (points) – water and ice temperature at 5 and –7·5 °C; Re = 9500, 12 700, 15 900 and 19 000. ■, duration of the acceleration phase. This figure is available in colour online at www.interscience.wiley.com/journal/espl

In order to study typical conditions of periglacial rivers in Siberia, the following conditions were considered: water temperature T_w = 5 to 20 °C, discharges Q = 5000 to 100 000 m^3 s^{-1}, ground ice temperature T_i = –5 to –80 °C. Variations in ice content of 20, 40 and 80% are also considered. The typical case T_L = 5 °C, T_i = –10 °C and Q = 10 000 m^3 s^{-1} is chosen as a reference.

According to the results of the constant-rate melting model (Costard *et al.*, 2003), the ablation rate increases with water temperature, ice temperature and discharge and decreases with ice content. The effects of the water temperature are predominant, followed by the effects of the discharge, the ice content and the ice temperature (Figure 6). Based on the reference case, the erosion rate can be multiplied by a factor of about four by an increase of water temperature from 5 to 20 °C or by an increase of the discharge from Q = 10 000 m^3 s^{-1} to 100 000 m^3 s^{-1}. An increase of the ice temperature from –80 to –5 °C only increases the erosion rate by a factor of 1·6, whereas the erosion rate is multiplied by a factor of 3 when the ice content varies from pure ice to 20%.

The variation of the duration of the acceleration phase with the different parameters can be summarized by a decrease of the duration of the acceleration phase when the erosion rate increases. Considering pure ice or permafrost at –10 °C, even with extreme variations of water temperatures, water discharges provide a very short acceleration phase, which lasts a few minutes (Figure 6). On the other hand, the duration time is very sensitive to the ice temperature. It is about 14 minutes for pure ice at –10 °C, but remains about 4 hours for pure ice at –80 °C. The longer acceleration phase duration of up to 4 hours corresponds to a permafrost temperature of –80 °C put into 5 °C water at a flowing rate of 5000 m^3 s^{-1}.

The ablation rate and the duration of the acceleration phase are nearly identical (about 2·4 mm s^{-1} and 1 minute) for a 10 000 m^3 s^{-1} discharge associated with 20 °C water temperature and 100 000 m^3 s^{-1} discharge associated with 5 °C water temperature. As in the field these parameters vary simultaneously, it is interesting to study the combined effects of their evolution on the thermal erosion process.

DOI: 10.1002/esp

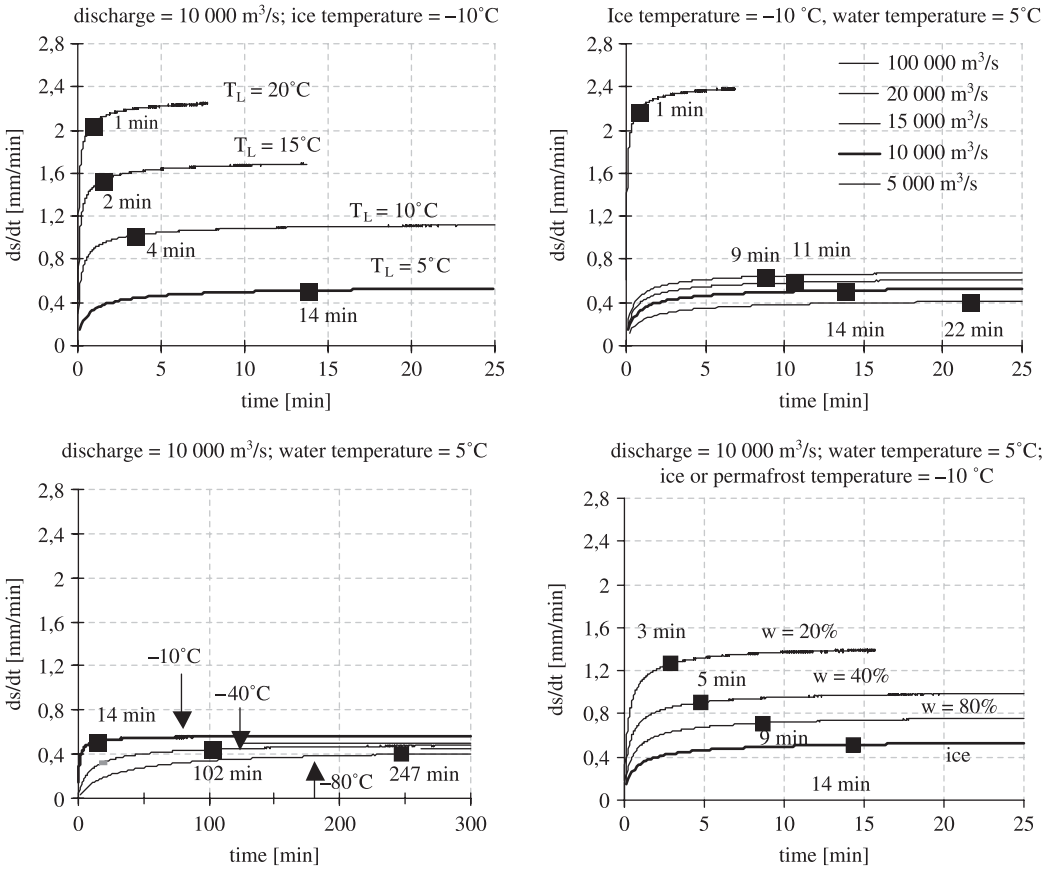

Figure 6. Applications to an arctic river. Effects of water temperature, discharge, ice temperature and ice content on the thermal erosion rate and the duration of the acceleration phase. Bold line, reference case. ■, duration of the acceleration phase.

Synthesis and Discussion

Water temperature and discharge can be represented by the heat flux exchanged by convection at the interface between the water flow and the permafrost (Equation (21) and Figure 7).

$$q = h(T_L - T_m) \tag{21}$$

where h is the convective heat transfer coefficient between the water flow and the permafrost, which depends on the discharges and the water temperatures (Equation (20)).

The convective heat flux (Equation (21)) appears more interesting because it may correspond to an infinity of combinations between water temperature and discharge (Figure 7). The convective heat flux will allow estimation of both the ablation rate and the duration of the acceleration phase (Figure 8(a), (b)), using our model of ablation. Therefore, we plot a diagram of the convective heat flux represented by isoflux lines as a function of the water temperature and the discharge (Figure 7). On the same diagram, we also plot the Lena basin and tributary data (water temperature and discharge), every ten days during the flood season. For instance, in the case of the Lena basin outlet, on 20 June, the water flow is characterized by a temperature equal to 4·4 °C and a discharge equal to 75 000 $m^3\ s^{-1}$ (in these conditions, the convective heat flux is about 5000 W m^{-2}).

As expected (Equation (21)), the heat flux increases when the water temperature and the discharge increase simultaneously from May to mid-June (Figure 7). By contrast, from June to July the water temperature is still increasing, while the discharge decreases by about 50%. During this increasing temperature stage (from May to 20 July for the Lena river and its tributaries), a positive trend of the heat flux is still observed. The maximum (12 000 and 14 000 W m^{-2} for the southern Lena sub basin and for the Lena basin outlet, respectively) of the heat flux occurs

DOI: 10.1002/esp

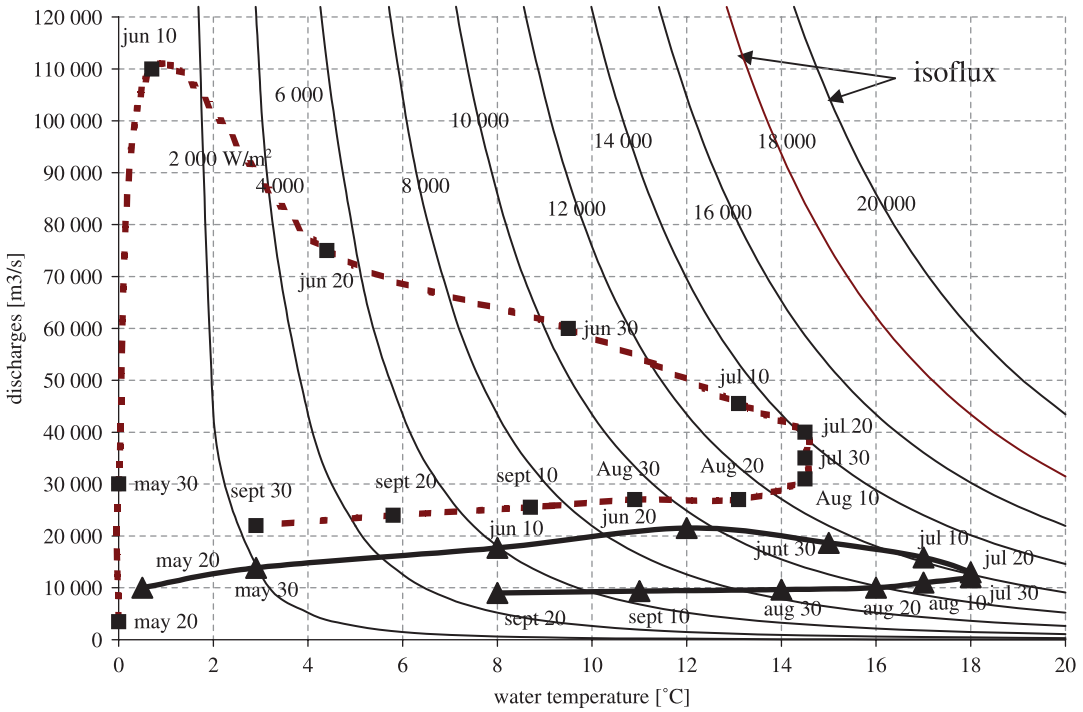

Figure 7. Diagram of heat flux versus discharge and water temperature. Fine line, isoflux (4000–20 000 W m^{-2}). ■, water mean temperatures and discharges in the Lena basin outlet (Yang *et al.*, 2002; Liu *et al.*, 2005); ▲, the southern Lena sub-basin (Aldan, Upper Lena, Vilui basin (Liu *et al.*, 2005). This figure is available in colour online at www.interscience.wiley.com/journal/espl

during July during the stable temperature stage when water reaches its maximum temperature. During a decreasing temperature stage (from 10 August to September), the heat flux decreases. From these considerations, it appears that the convective heat flux evolution mainly depends on the water temperature evolution for Siberian rivers during the flood season.

The heat flux variation for the Aldan, Upper Lena and Vilui river is similar to that of the Lena basin outlet. The difference in the heat flux peaks for these rivers is not significant (about 2000 W m^{-2}) and the delay of about 10 days observed for the Lena basin outlet compared to the southern Lena sub-basin is due to the latitudinal difference in climatic variables, such as air temperature. The higher values of water temperatures for the southern Lena sub-basin are compensated by the higher values of the discharges for the Lena basin outlet.

With regards to specific heat flow, the application of the model of variable rate to pure ice or permafrost should allow determination of the ablation rate and the duration of the acceleration phase (Figure 8(a), (b)). This figure is drawn point by point from the ablation rate and the duration of the acceleration phase for a given convective heat flux. Two types of curve compose the diagrams: one represents the isoflux and the other one represents the isotherms of ice or permafrost.

The Lena basin outlet and the southern Lena sub-basin cases are represented in these diagrams. For these applications, the convective heat flux is calculated from the water temperatures.

The greater the convective heat flux, the greater the erosion rate and the smaller the duration of the acceleration phase (Figure 8(a), (b)). For ice at −10 °C, the maximum ablation rate is about 2·6 mm min^{-1} (3·7 m day^{-1}) and the duration of the acceleration phase is about 10 minutes, considering a typical maximum value of the convective heat flux for arctic rivers (14 000 W m^{-2}, Figure 7). For a smaller value of q (= 4000 W m^{-2}), the ablation rate is about 0·7 mm min^{-1} (1 m day^{-1}) and the duration of the acceleration phase is about 3 hours.

The most favourable conditions to achieve the longer acceleration phase are obtained for the smaller values of the erosion rate at the beginning (early May) or at the end (October) of the flood season. For example, considering a small thermal erosion rate of 0·06 mm min^{-1} (early May), the acceleration phase lasts about 14 days.

Only a weak impact of ice temperature on the ablation rate and the acceleration phase is noted. Thermal erosion of pure ice is smaller and the acceleration phase is longer compared with the permafrost.

DOI: 10.1002/esp

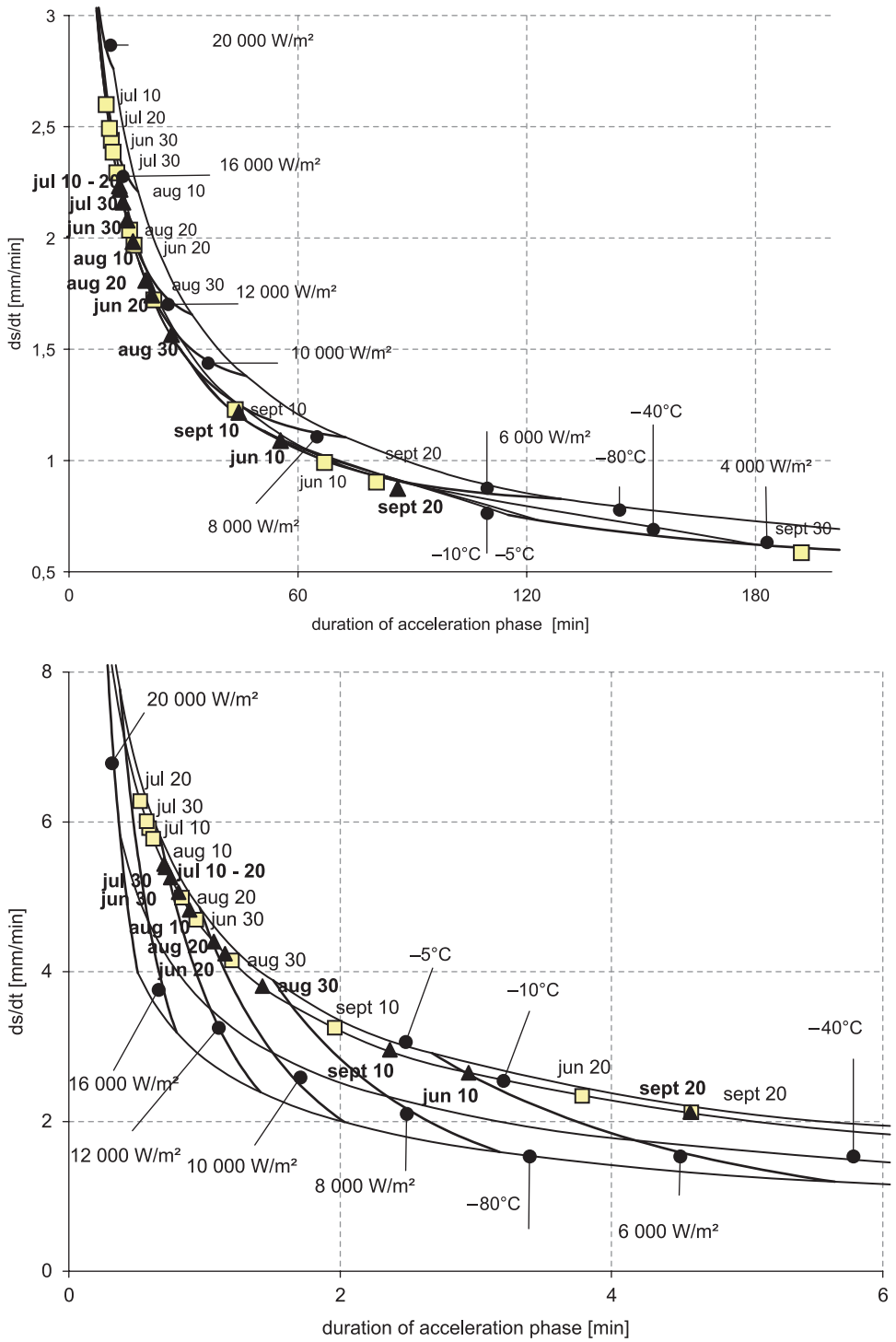

Figure 8. Diagram of ablation rate and duration of acceleration phase for various convective heat fluxes and ground temperatures. For pure ice (a) and for permafrost (b) with ice content equal to 20%. Bold line: isoflux (4000–20 000 W m^{-2}), fine line: isothermal (–10 to –80 °C). Case of the Lena basin outlet (▲) and case of the Lena tributaries (□) (Aldan, Upper Lena, Vilui basin) (Liu *et al.*, 2005). This figure is available in colour online at www.interscience.wiley.com/journal/espl

DOI: 10.1002/esp

Summary and Conclusion

Along the Lena river, riverbank erosion can reach up to 40 m per year due to thermal erosion of frozen riverbanks in permanent contact with water from the river. The process is linked to the following parameters: water and ice temperature, discharge and level of ice content in the frozen soil. A model with a constant-rate melting supported by experiments undertaken in a cold room was previously used to study the thermal erosion process (Costard *et al*., 2003). The constant-melting-rate model does not take into account the acceleration phase occurring at the beginning of the thermal erosion process. A more general model at variable rate, based on the integral method (Goodman, 1958), has been developed.

The mathematical statement of ice or permafrost thermal erosion in permanent contact with turbulent water flow has been formulated. The expressions of the melting thickness and the ablation rate have been obtained by the integral method and validated by experiments on ice samples. Result show clearly that an acceleration phase occurs at the beginning of the process. The duration of this acceleration phase is analysed and quantified.

The model has contributed to elucidate the relative contribution of each parameter during the thermal erosion process. Water temperature, discharge and ice content all increase the ablation rate, whereas the level of ice content in the soil tends to slow down the thermal erosion process. The effects of water temperature are predominant. The acceleration phase lasts longer for a low ablation rate. By extrapolating, a low and long acceleration phase results from low water temperature, a low discharge (low convective heat flux) and a low ice temperature, but a relatively high level of ice content in the frozen river banks. From these results, it appears that the heat fluxes along the river banks are almost identical for the Lena basin outlet and for the southern Lena basin because higher values of water temperatures for the southern Lena sub-basin are compensated by the higher values of the discharges for the Lena basin outlet. In early May, just before the breakup, the acceleration phase lasts 14 days when the water temperature is close to the melting point (low heat flux).

Recent climatic change is deeply influencing the river functioning. The progressive increase of the active layer depth (Fedorov and Konstantinov, 2003) since the early 1980s conducts to a most important groundwater supply in the river bed (Peterson *et al*., 2002). From our studies, the water temperature is a quite important parameter. Further studies will take into account the possible effect of the global warming on the thermal erosion rate using our model. One possibility is that increasing winter and spring discharges together with water temperature increases could accelerate the river bank retreat and therefore partly destabilize the fluvial dynamics.

Acknowledgements

We thank D. Gobin for helpful discussions on the numerical approach to the problem. This work is supported by the programme RELIEFS from CNRS-INSU and GDR Arctic.

References

Aguirre-Puente J, Costard F, Posado-Cano R. 1994. Contribution to the study of thermal erosion on Mars. *Journal of Geophysical Research* **99**: 5657–5667.

Anisimova NP, Nikitina NM, Piguzova UM, Shepelyev VV. 1973. Water sources of Central Yakutia – Guidebook. In *Proceedings, II International Conference on Permafrost*, Yakutsk, USSR. National Academy of Sciences: Washington, DC.

Antonov S. 1960. Delta reki Leny. Trudy Okeanographitcheskiy Comissyi. *Akademii. Nauk. SSSR* **6**: 25–34.

Are Fe. 1983. Thermal abrasion of coasts. In *Proceedings of the Fourth International Conference on Permafrost*, Alaska. National Academy Press: Washington, DC; 24–28.

Bejan A. 1993. *Heat Transfer*. Wiley: New York.

Carslaw HS, Jaeger JC. 1959. In *Conduction of Heat in Solids*. Oxford University Press: Oxford; 282–296.

Costard F, Aguirre-Puente J. 1999. Martian fluvial–thermal erosion: laboratory simulation. *Journal of Geophysical Research* **104**: 14.091–14.098.

Costard F, Dupeyrat L, Gautier E, Carry-Gailhardis E. 2003. Fluvial thermal erosion investigation along a rapid eroding river bank: application to the Lena river (central Siberia). *Earth Surface Processes and Landforms* **29**: 1349–1359.

Fedorov A, Konstantinov P. 2003. Observations of surface dynamics with thermokarst initiation, Yukechi site, Central Yakutia. In *Permafrost*, Philips M, Springman S, Arenson LU (eds). Proceedings of International Permafrost Conference, Zurich. A. A. Balkema Publishers: Lisse; 239–243.

Gautier E, Brunstein D, Costard F, Lodina R. 2003. Fluvial dynamics in a deep permafrost zone: the case of the middle Lena river (Central Yakutia). In *Proceedings of International Permafrost Conference*, Zurich; 6.

Gautier E, Costard F. 2000. Les systèmes fluviaux à chenaux anastomosés en milieu périglaciaire: la Léna et ses principaux affluents (Sibérie centrale). *Géographie Physique et Quaternaire* **54**: 327–342.

DOI: 10.1002/esp

Goodman TR. 1958. The heat-balance integral and its applications to problems involving a change phase. *Transaction ASME* **80**: 335–342.

Gordeev VV, Sidorov IS. 1993. Concentrations of major elements and their outflow into the Laptev Sea by the Lena river. *Marine Chemistry* **43**: 33–45.

Ho CD, Yeh HM, Wang WP, Wang JK. 2000. *International Communications in Heat and Mass Transfer* **27**: 785–794.

Jahn A. 1975. *Problems of the Periglacial Zone*. Warzawa: Washington, DC.

Landau HG. 1950. Heat conduction in a melting solid. *Quarterly of Applied Mathematics* **8**: 81–95.

Liu B *et al*. 2005. Long-term open-water season stream temperature variations and changes over Lena River Basin in Siberia. *Global and Planetary Change* **48**: 96–111.

Lunardini VL, Zisson JR, Yen YC. 1986. *Experimental Determination of Heat Transfer Coefficients in Water Flowing over Horizontal Ice Sheet*, CREEL Report 86-3. US Army Cold Regions Research and Engineering Laboratory.

Peterson BJ, Holmes RM, McClelland JW, Vörösmarty CJ, Lammers RB, Shiklomanov AI, Shiklomanov IA, Rahmstorf S. 2002. Increasing river discharge to the Arctic Ocean. *Science* **298**: 2171–2173.

Péwé TL. 1991. *Origin and Character of Loesslike Silt in Unglaciated South-Central Yakutia, Siberia, USSR*, US Geological Survey Professional Paper 1262.

Shiklomanov A, Lammers RB, Peterson BJ, Vörösmarty CJ. 2000. The dynamics of river water inflow to the Arctic Ocean. In *The Freshwater Budget of the Arctic Ocean*, Proceedings of the NATO Advanced Research Workshop, Tallin, Estonia, 1998, Lewis EP, Lemke P, Prowse TE, Wadhams P (eds). Kluwer: Norwell, MA; 281–296.

Soodak H. 1943. *Effects of Heat Transfer Between Gases and Solids*, PhD thesis. Duke University: Durham, NC.

Yamskikh AF, Yamskikh AA, Brown AG. 1999. Siberian-type Quaternary floodplain sedimentation: the example of the Yenisei river. In *Fluvial Processes and Environmental Change*, Brown AG, Quine TA (eds). Wiley: Chichester; 241–252.

Yang D, Douglas LK, Hinzman L, Zhang T, Ye H. 2002. Siberian Lena River hydrologic regime and recent change. *Journal of Geophysical Research* **107**: 4694. DOI: 10.1029/2002JD002542